Available online at www.sciencedirect.com
ScienceDirect
Cement and Concrete Research 37 (2007) 151 – 160
Cement and Concrete Research

Experimental limitations regarding the formation and characterization of uranium-mineral phases in concrete waste forms

Dawn M. Wellman [a,*], Shas V. Mattigod [a], Bruce W. Arey [a], Marcus I. Wood [b], Steven W. Forrester [c]

[a] Pacific Northwest National Laboratory, Applied Geology and Geochemisty, PO Box 999, K6-81, Richland, WA 99354, USA
[b] Fluor Hanford, 2420 Stevens Center, Richland, WA 99352, USA
[c] Department of Geology, Washington State University, Pullman, WA 99164, USA

Received 20 January 2006; accepted 2 November 2006

Abstract

Predicting the fate of low-level radioactive waste (LLW) requires understanding radionuclide–waste form interactions. Concrete encasement is one method being considered for containment of LLW. The formation of uranium-mineral phases has been investigated in simulated concrete pore fluids and waste forms. X-Ray diffraction analyses of uranium precipitates from concrete pore fluids suggest uranium salts and -silicates are solubility-limiting phases. Scanning electron microscopy-energy dispersive spectroscopic analyses of uranium-spiked concrete suggest that under conditions both under-saturated and over-saturated with respect to the formation of uranium phases, uranyl-oxyhydroxide phases precipitate within the initial two weeks. Uranyl-silicate phases form after approximately one month and uranyl-phosphate phases provide a significant contribution to uranium retention in concrete waste forms after two months. This investigation demonstrates the importance of 1) studying the interaction of uranium in the complete matrix (i.e., concrete matrix versus pore fluids) and 2) formation of uranium-mineral phases on the retention of uranium within concrete waste forms.

Keywords: Waste management (E); Radioactive waste (E); Concrete (E); Portland cement (D); Uranium

1. Introduction

To predict the long-term fate of low-level waste forms it is important to understand how radionuclides behave within and interact with the waste form. Concrete encasement is one method being considered for containment of low-level radioactive wastes. Concrete is expected to act as a hydrologic intrusion barrier to isolate the waste package from the environment. Failure of concrete waste packages may result in water intrusion and consequent leaching of contaminants into the surrounding subsurface environment via diffusion and/or advective flow.

Uranium is a significant component and long-term dose contributor in low-level radioactive waste [1,2]. Sorption of uranium to components of cementitous materials has been the subject of several investigations, including studies of metal oxides [3–5], carbonate-rich sediments and minerals [6–10], iron-bearing minerals [11,12], aluminum oxide [13], silicon dioxide [14,15], and concrete-specific components such as calcium-silicate-hydrates [16–18] and calcium-oxides [15]. Sutton et al. [21] suggested an apparent two-stage sorption mechanism attributed to surface complexation of uranium with siloxyl groups in grout. Sylwester et al. [19] supported this hypothesis utilizing X-ray absorption fine-structure spectroscopy and X-ray absorption near-edge spectroscopy, demonstrating that uranyl interacts with concrete components (i.e., SiO_2) through inner-sphere bonding mechanisms by sharing equatorial oxygen atoms with the mineral surface. This is significant in terms of uranium chemistry and retention in concrete waste forms for two reasons. First, in general, inner-sphere sorption complexes, relative to other mechanisms of sorption, are the most stable sorptive complexes [20]. Second, sorption occurring via inner-sphere complexes is believed to be an important precursor step in surface precipitation of uranyl minerals [21]. This suggests long-term immobilization of uranium within concrete waste forms may occur through the formation of uranium-mineral phases.

* Corresponding author. Tel.: +1 509 375 2017.
E-mail address: dawn.wellman@pnl.gov (D.M. Wellman).

0008-8846/$ - see front matter © 2006 Elsevier Ltd. All rights reserved.
doi:10.1016/j.cemconres.2006.11.004

The high pH conditions of grout material (pH ~ 12) limits the solubility of uranium by forming uranyl-oxides, uranyl hydroxides, and uranate salts [22–30]. However, the solubility of uranium in concrete waste forms has generally been investigated from under-saturated, model solutions [15,31–33]. Glasser et al. [33] and Atkins et al. [32] examined the solubility of uranium in the model Ca–UO_3–H_2O system, demonstrating the importance of calcium and sodium uranate phases. The results of this investigation provided valuable information regarding the formation of calcium and sodium uranate phases. However, relevant to concrete waste forms, the model system neglects the chemical complexities associated with concrete pore waters given the absence of the dominant component of concrete, SiO_2. Brownsword [31] investigated the solubility of uranium in concrete equilibrated pore waters. Results demonstrated the solubility of uranium under these conditions is equal to or lower than the solubility of sodium and calcium uranates and, therefore, concluded the solubility-limiting phase corresponded to calcium and/or sodium uranates. However, no additional support or characterization of the solid phases precipitated from concrete equilibrated pore waters was provided to defend this conclusion. Glasser [34] noted the difficulty of differentiating the solubility-limiting phases for uranium in complex matrices such as concrete waste forms. Correlating the solubility of uranium in concrete equilibrated pore waters to calcium and/or sodium uranates without direct evidence is subject to debate within such a complex chemical system. To this end, Moroni and Glasser [15] investigated the model CaO–UO_3–SiO_2–H_2O system and illustrated the significance of uranyl silicate minerals on the retention of uranium within concrete matrices. They noted that the solubility of uranium is not solely a function of uranium loading; rather, it is controlled by the nature of uranium-bearing precipitates and within any phase compatibility region, is ideally independent of the amount of each phase.

To quantify the long-term stability of uranium in concrete waste forms, solubility studies have been conducted on proposed uranium-mineral phases that have been predicted via geochemical modeling to be the dominant controls on uranium [29–35]. However, a limited range of experimental conditions [31] and the presence of multiple uranium phases have complicated experimental solubility results [31,33,35]. This in conjunction with geochemical predictions rather than experimental determination of uranium phases hinders the accuracy of predictions regarding the long-term fate of uranium in concrete waste forms [36].

Although previous studies provide necessary information regarding the reactions of uranium with various cementitous materials, concrete is a continuously reacting solid, and its component phases continue to change over hundreds of years, albeit very slowly [37 38]. Therefore, to accurately assess the performance of concrete for radionuclide encasement, it is necessary to understand the interactions between radionuclides and the concrete matrix to identify *in situ* the formation of uranium phases. We present results of two data sets, the first of which were generated to characterize uranium-solid phases precipitated from concrete pore waters. Secondly, we present the results of an *in situ* microscopic investigation elucidating the uranium-mineral phases controlling the long-term fate of uranium within concrete waste forms. Comparison of *ex situ* pore water studies, and *in situ* phase identification illustrates the limitations of predicting solubility-limiting phases for complex contaminants such as uranium in pore fluids versus concrete matrices. Results of this investigation further illustrate the necessity to conduct detailed, *in situ* analyses to understand the long-term mechanisms of retention for uranium in complex matrices such as concrete.

2. Experimental

2.1. Preparation of uranium-spiked Portland concrete pore water solutions

Ewart et al. [39] measured the elemental compositions of pore waters equilibrated with a series of Portland cement compositions: sulfate resistant Portland cement/limestone (SRPC/L), ordinary Portland cement/blast furnace slag/limestone (OPC/BFS/L), blast furnace slag/ordinary Portland cement (BFS/OPC), ordinary Portland cement/limestone (OPC/L), and Harwell. Based on this data, a series of synthetic cement leachates were prepared with 18 MΩ deionized water and reagent grade chemicals from Aldrich Chemicals: calcium chloride [$CaCl_2{\cdot}2H_2O$], magnesium chloride [$MgCl_2{\cdot}6H_2O$], calcium sulfate [$CaSO_4$], sodium hydroxide [NaOH], calcium carbonate [$CaCO_3$], calcium hydroxide [$Ca(OH)_2$], silicic acid [$SiO_2{\cdot}2H_2O$], and aluminum nitrate [$Al(NO_3)_3{\cdot}9H_2O$] (Table 1).

Two sets of solutions were prepared by adding 20 mL of 110 mM uranyl nitrate [$UO_2(NO_3)_2{\cdot}6H_2O$] (Alfa Aesar) dropwise to 60 mL of each synthetic leachate solution, while stirring under ambient conditions. The total uranium concentration was $\sim 2.7 \times 10^{-3}$ M, which is greater than the saturation-limiting concentration established by Ewart et al. [39]. However, precipitation was visibly

Table 1
Chemical composition of Portland cement-equilibrated waters; concentrations are in molarity

Cement	Ca	Na	Mg	Cl	SO_4^{2-}	CO_3^{2-}	Al	Si	pH
SRPC/L	6.7×10^{-3}	2.0×10^{-4}	$<8\times10^{-8}$	4.0×10^{-5}	4.0×10^{-5}	8.5×10^{-5}	7.4×10^{-4}	5.3×10^{-6}	12.5
9:1 BFS/OPC	6.8×10^{-3}	3.4×10^{-3}	4.7×10^{-7}	6.2×10^{-5}		1.0×10^{-4}	8.0×10^{-5}	2.3×10^{-5}	12.2
OPC/BFS/L	6.7×10^{-3}	5.0×10^{-3}	$<8\times10^{-7}$	2.4×10^{-3}	6.0×10^{-3}	2.8×10^{-4}	9.5×10^{-5}	7.0×10^{-4}	12.1
OPC/L	2.0×10^{-2}	8.3×10^{-4}	$<4.\times10^{-8}$	9.0×10^{-5}	1.0×10^{-5}	2.0×10^{-5}	1.0×10^{-5}		12.0
Harwell	1.0×10^{-2}	5.0×10^{-5}	5.0×10^{-6}	2.0×10^{-3}	3.0×10^{-3}	3.0×10^{-5}			12.0

[39].

Table 2
Material specifications and composition

Material	Specifications	Specified field mix	Mass normalized specification design
Cement	Portland Type I or Type I/II sulfate-resistant cement	381 kg/m^3	0.27
Fly ash	Class F fly ash; nominal 15% of cement by volume	54 kg/m^3	0.04
Coarse aggregate	2 cm nominal size	55% by volume	0.04
Fine aggregate	Sand	45% by volume	0.51
Water	Nominal water: cement ratio: 0.4	399 kg/m^3	0.10
Steel fiber	Deformed Type I, nominal length 2.5–3.8 cm	59 kg/m^3	0.04
Air content		6.0±1.5%	

evident after adding ~1 mL of uranyl nitrate solution, which is well below the limiting concentration of 10^{-5} M. One set of solutions was stirred for 2 h under ambient conditions; the second set of solutions was heated at 90 °C for 24 h to evaluate the effects of thermal heating on uranium phase formation exhibited by cementitious materials. Precipitates were collected via vacuum filtration with 0.45 μm Nalgene disposable filters.

2.2. Preparation of uranium-spiked Portland cement

The specified composition for concrete waste encasement has been described in *Specification for Concrete Encasement for Contact-Handled Category 3 Waste*[1] (Table 2). Based on this composition, laboratory-scale test specimens were prepared (Table 3). Because of the required small dimensions of laboratory test specimens, the size of the coarse aggregate was proportionately reduced from 2 cm to a particle size ranging from 2.83 mm to 2 mm in the laboratory mix. The dimensions of the scaled-down steel fibers used in the laboratory mix consisted of Bekaert Dramix brand deformed steel wire fibers, cut to a nominal length of 8 mm and void of any surface coatings. The deformed end portions were retained for use in the concrete mixture and the straight middle sections of the fibers were discarded. The volumes of the water-reducing agent, Polyheed 997 (Master Builders), and the air-entraining agent, MB AE 90 (Master Builders), were not included in the normalization calculations because of their negligible contribution to the overall mix volume. Although the steel fibers could serve as a reductant for uranium, no change in redox state was detected during the investigation.

Based on the nominal laboratory-scale composition, composition #1, a series of 200 mL batches was prepared, with varying steel and aqueous uranium compositions (Table 4). Uranium-spiked samples were prepared by dissolving the uranium within the water fraction of the concrete composition to promote homogeneous distribution of uranium within the concrete waste package. The uranium concentrations were chosen such that the 10^{-3} M uranium spike yielded an overall concentration within the concrete matrix of 30 ppm, which is under-saturated with respect to uranium and within the concentration range in which sorption is believed to be the controlling mechanism for uranium retention. The 0.1 M uranium spike gives an overall concentration within the concrete matrix over-saturated with respect to uranium-solid phases of 3000 ppm. The concrete was hand mixed in a stainless steel bowl with a stainless steel whisk for approximately 10 min, divided into three equal sub-samples, loaded into zip-lock bags, pressed into flat sheets, and sealed. The samples were allowed to set for predetermined time intervals of two weeks to three months prior to analysis.

[1] Unpublished Report, Waste Management, 1998.

2.3. X-Ray diffraction

Solids precipitated from aqueous solutions were characterized using X-ray diffraction (XRD), which is a technique commonly used to identify crystalline minerals that are ≤5% (by weight) of the bulk composition. Before mounting, a representative sample of the bulk material was ground, using an agate mortar and pestle, to improve the diffraction patterns. X-Ray diffraction data of uranium-pore water precipitates were obtained at 45 kV and 40 mA using a Scintag® automated powder diffractometer (Model 3520) with nickel-filtered copper radiation, $CuK_\alpha = 1.54$ Å. The samples were analyzed over the 2-theta? (2θ) range from 2° to 65°, using a step size of 0.04° and a two-second count time at each step.

2.4. Scanning electron microscopy-energy dispersive spectroscopy

Precipitates from uranium-laden pore waters and uranium-spiked concrete samples were mounted on aluminum planchettes and carbon-coated under a vacuum to provide sufficient conductivity and to mitigate surface charging. Micrographs

Table 3
Laboratory-scale material specification and composition

Material	Material specifications for field mix	Mass normalized laboratory design	Material specifications used in revised laboratory mix comparison
Cement	Portland Type I or Type I/II sulfate-resistant cement	0.27	Portland Type I and II
Fly ash	Class F fly ash; nominal 15% of cement by volume	0.04	Class F fly ash; nominal 20% of cement by volume
Coarse aggregate	2 cm nominal size	0.04	2.83–2 mm
Fine aggregate	Sand	0.51	Sand<2 mm
Water	Nominal water: cement ratio: 0.4	0.10	Water-to-cement ratio: 0.5
Steel fiber	Deformed Type I, nominal length 2.5–3.8 cm	0.04	Deformed, nominal length 8 mm
Polyheed 997		0.00375	Water-entraining agent
Air content	6.0±1.5%	6.0±1.5%	–

Table 4
Concrete compositions

Normalized laboratory design	Comp. #1	Comp. #2	Comp. #3	Comp. #4	Comp. #5	Comp. #6	Comp. #7
0.27	Cement	Cement	Cement	Cement	Cement	Cement	Cement
0.04	Fly ash	Fly ash	Fly ash	Fly ash	Fly ash	Fly ash	Fly ash
0.04	Coarse aggregate	Coarse aggregate	Coarse aggregate	Coarse aggregate	Coarse aggregate	Coarse aggregate	Coarse aggregate
0.51	Fine aggregate	Fine aggregate	Fine aggregate	Fine aggregate	Fine aggregate	Fine aggregate	Fine aggregate
0.10	Water	10^{-3} M [a] uranium (aq)	10^{-3} M [a] uranium (aq)	10^{-3} M [a] uranium (aq)	0.1 M [b] uranium (aq)	0.1 M [b] uranium (aq)	0.1 M [b] uranium (aq)
0.04	Steel fiber	–	Steel fiber	Iron filings	–	Steel fiber	Iron filings

[a] 10^{-3} M spike = 30 ppm concentration in concrete.
[b] 0.1 M spike = 3000 ppm concentration in concrete.

were obtained with a JEOL 840 scanning electron microscope equipped with a Robinson 6.0 backscattered detector and GATAN DM software. Compositional information was obtained with an Oxford ISIS 300 series Energy Dispersive Spectrometer with Oxford ISIS 300 version 3.2 software. The beam conditions were 20 kV acceleration and a 1 nA beam current.

3. Results and discussion

3.1. Precipitates from uranium-spiked pore waters

Fig. 1 displays XRD patterns obtained from solids precipitated under ambient conditions in the uranium-spiked pore water after a two-hour reaction period. XRD patterns display few reflections, indicating the phases were predominantly amorphous in nature; yet, a number of significant features are present within the XRD patterns. All of the patterns, with the exception of BFS/OPC, display a small peak at 5.58° 2θ, which is a characteristic low-angle peak of ettringite [$Ca_6Al_2(SO_4)_3(OH)_{12}\cdot 26H_2O$], a calcium-aluminum-sulfate compound commonly found in cement. BFS/OPC lacks sulfate as a compositional element; therefore, ettringite was not observed within this precipitated phase. Additionally, comparison of the intensity of this reflection can be directly correlated to the sulfate concentration within the composition and decreases accordingly.

Uranium precipitates from all compositions, except OPC/BFS/L, display a small, amorphous, low-angle peak within the region of 11.8 to 12.1° 2θ, Fig. 1), which is a major reflection for both becquerelite and meta-schoepite. The precipitate from OPC/BFS/L displays a sharp peak within this region. However, the lack of additional reflections, characteristic of either becquerelite or meta-schoepite, precludes making a clear distinction regarding the dominant phase controlling the solubility of uranium based solely on diffraction patterns. Additionally, all precipitates display a broad peak within the region of approximately 25 to 29° 2θ. Both becquerelite and meta-schoepite display a series of minor reflections within this region; however, calcium and sodium diuranate dihydrate also have major reflections within this region. The significance of becquerelite and meta-schoepite phases in concrete waste forms has been noted [15,30,32–34]. Likewise, a number of investigations have previously suggested diuranate dihydrate salts as predominant phases for controlling the solubility of uranium under conditions relevant to concrete pore waters [15,32,40]. Without defined reflections or further characterization of the solid phase, the dominant control on the solubility of uranium cannot be conclusively identified.

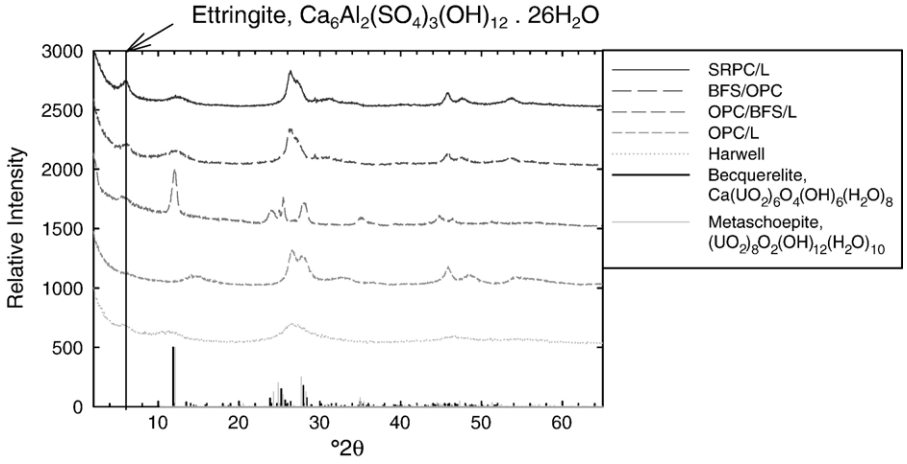

Fig. 1. X-ray diffraction patterns from Portland cement leachate-U(VI) precipitates at room temperature after two weeks.

After one year, all compositions, with the exception of BFS/OPC, exhibited a characteristic low-angle reflection, 5.58° 2θ, of ettringite (Fig. 2), the intensity of which had not changed given the prolonged reaction period. All precipitates display a broad peak within the region of 11.8 to 12.1° 2θ. Both becquerelite and meta-schoepite display reflections in this region, and no clear distinction between the two solid phases was possible (Fig. 2). XRD patterns for all solids also display a large amorphous hump centered at approximately 20° 2θ, suggestive of SiO_2 (am). Also prominent in all patterns, except SRPC/L, is a sharp reflection at 29° 2θ due to the presence of calcite.

X-Ray diffraction results presented here illustrate the significant challenges of discerning uranium-solid phase(s) in complex matrices. The structural similarity of uranium-solid phases and formation of additional phases such as calcium phases typically present in concrete, complicate interpretation of powder diffraction data. This precludes conclusive identification of solid phases precipitated from concrete pore waters based solely on XRD analyses. Short-term batch tests, commonly utilized to elucidate the solid phases controlling the long-term retention of uranium within concrete, oversimplify the complexities of uranium chemistry especially when coupled with constantly changing conditions of concrete pore waters. XRD results from batch tests conducted under ambient conditions for a period of 2 h versus one year suggest changes in the chemical composition of the precipitate, but little change in the crystallinity of the precipitate. Although the composition of cement is dominated by calcium hydroxide and silicate hydrates [38], as the concrete ages into a more complicated polymeric framework, contaminants such as uranium may diffuse and react, significantly altering the presumed retention mechanism based on the results from short-term investigations [41].

Precipitates from uranium-laden pore waters, formed at 90 °C, yield XRD patterns that indicate a significant increase in crystallinity, and the formation of phases that did not form under ambient conditions (Table 5, Fig. 3). Notably absent from the XRD patterns are the major peaks for becquerelite and/or meta-schoepite within the regions of 11.8 to 12.1° 2θ, which were evident in precipitates formed under ambient conditions. Yet, a broad peak, indicative of the amorphous nature of the material remains evident in all patterns from 25° to 30° 2θ, which is within the region where multiple reflections are displayed for schoepite, becquerelite, and calcium uranium oxides. However, no clear distinction between the solid phases can be inferred based solely on XRD data. Moreover, because the concentration of uranium is limited relative to the major elemental components of the concrete matrix, it is plausible that the increased precipitation of calcium phases (Table 5), typically present in concrete, is masking reflections from the minor inclusions of uranyl-phases. Comparison of the results presented here for short-term batch tests conducted under ambient conditions versus those conducted at 90 °C illustrate that an increase in temperature increases the crystallinity of the precipitate, but may also afford changes in the chemical composition of the precipitated phase(s). Additionally, the behavior of radionuclides such as uranium may be significantly different in thermally treated concrete waste forms.

Table 5
Mineralogical composition of 90 °C precipitates determined by XRD peak-fitting

	OPC	Harwell	BFS/OPC	SRPC	OPC/BFS
Portlandite [$Ca(OH)_2$]	X	X	X		Trace
Thermonatrite [$Na_2CO_3 \cdot H_2O$]	X			X	Trace
Halite [NaCl]		X			
Aragonite [$CaCO_3$]		X	X		Trace
Phlogopite [$KMg_3(AlSi_3O_{10})(OH)_2$]		X			
Calcite [$CaCO_3$]			X	X	X

3.2. In situ characterization of uranium precipitates in concrete

3.2.1. 10^{-3} M uranium-spiked concrete samples

Fig. 4a displays scanning electron microscopy–energy dispersive spectroscopy (SEM–EDS) analyses of concrete samples containing 30 ppm uranium after a two-week reaction period. The SEM image reveals a small area of concentrated uranium. The occurrence of these regions was minimal, and the majority of the uranium appeared to have been equally distributed throughout the concrete matrix. EDS analysis of the concentrated

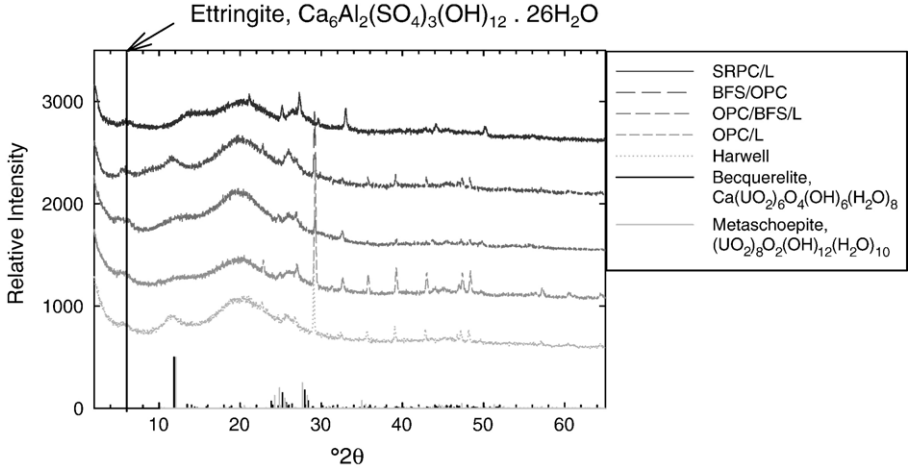

Fig. 2. X-ray diffraction patterns from Portland cement leachate-U(VI) precipitates at room temperature after one year.

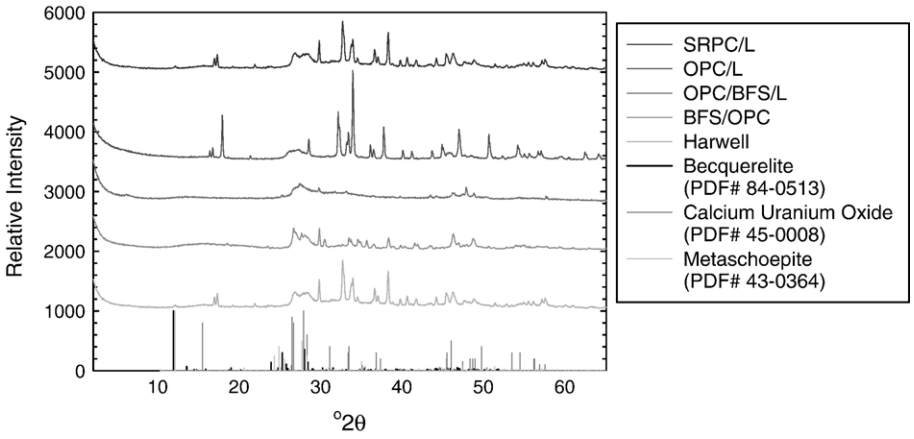

Fig. 3. X-ray diffraction patterns from Portland cement leachate-U(VI) precipitates at 90 °C after 2 h.

regions indicated the major components to be uranium and oxygen (Fig. 4b). Sutton et al. [21] previously noted that even under high pH conditions present in grout, where both the surface sites and uranyl hydroxide ions are anionic, sorption is observed via an inner-sphere complexation between the hydroxide bridging the uranyl hydroxide ions and the hydroxylated grout surfaces. Additional Extended X-ray Absorption Fine Structure/X-ray absorption near-edge structure (EXAFS/XANES) studies have supported the observed formation of inner-sphere, bidentate-bound uranium ions to silicate surfaces [42–44]. This is significant for two reasons: (1) inner-sphere sorption complexes, relative to other mechanisms of sorption, are the most stable sorptive complexes [20] and (2) sorption occurring via inner-sphere complexes is believed to be an important precursor step in surface precipitation of uranyl minerals [21].

Although, uranium was initially observed to be evenly distributed throughout the concrete matrix on a microscopic scale, after a period of one month, SEM analyses display a cluster of uranyl phases (Fig. 5) (similar observations were previously noted by Maroni and Glasser [15]). EDS analyses indicate a significant oxygen content and a minor silicon concentration. Based on the silica–oxygen–uranium ratio, identifying the uranyl phase solely as a uranyl-silicate phase results in an excess of uranium and oxygen. This indicates the phase is a mixed uranyl-oxyhydroxide/silicate phase, possibly uranophane mixed with becquerelite and/or meta-schoepite, as suggested by XRD results of uranium pore water precipitates. These results suggest advanced uranyl-mineral phases may act as a long-term control of uranium even at very low uranium concentrations and agree with results of previous investigations which suggest the solubility of uranium is not primarily a function of uranium loading. Rather, the solubility is controlled by the nature of the uranium precipitates [15]. The apparent formation of uranyl-oxyhydroxide/silicate phases after one month supports the hypothesis that sorption through inner-sphere mechanisms is a precursor for precipitation of uranium-mineral phases [19,21].

3.2.2. 0.1 M uranium-spiked concrete samples

Scanning electron microscopy images of concrete samples containing 3000 ppm uranium revealed extensive formation of

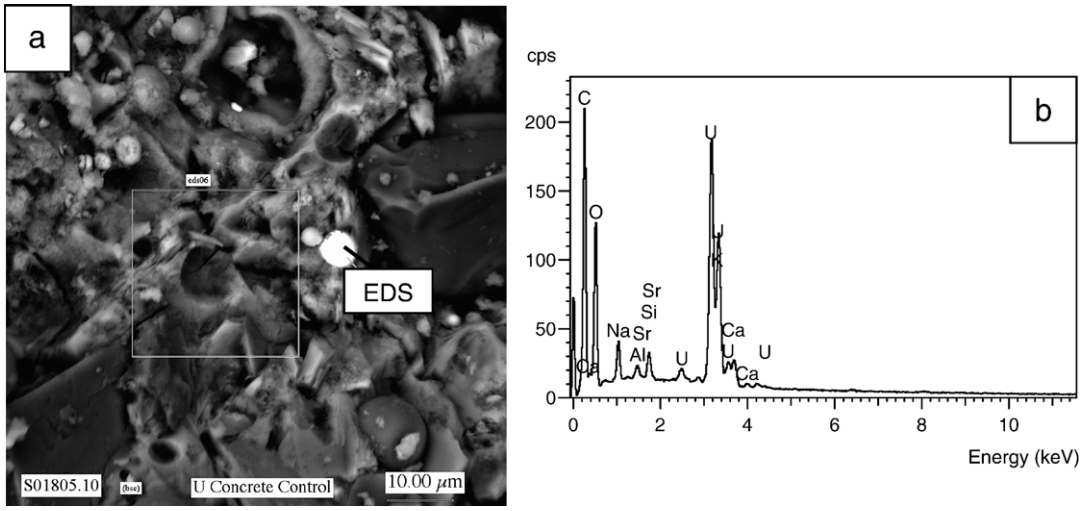

Fig. 4. (a) Scanning-electron microscopy photomicrograph of uranium phase formed within OPC spiked with 10^{-3} M uranium after two weeks. (b) Energy dispersive pattern suggests the phase is a uranyl-oxyhydroxide.

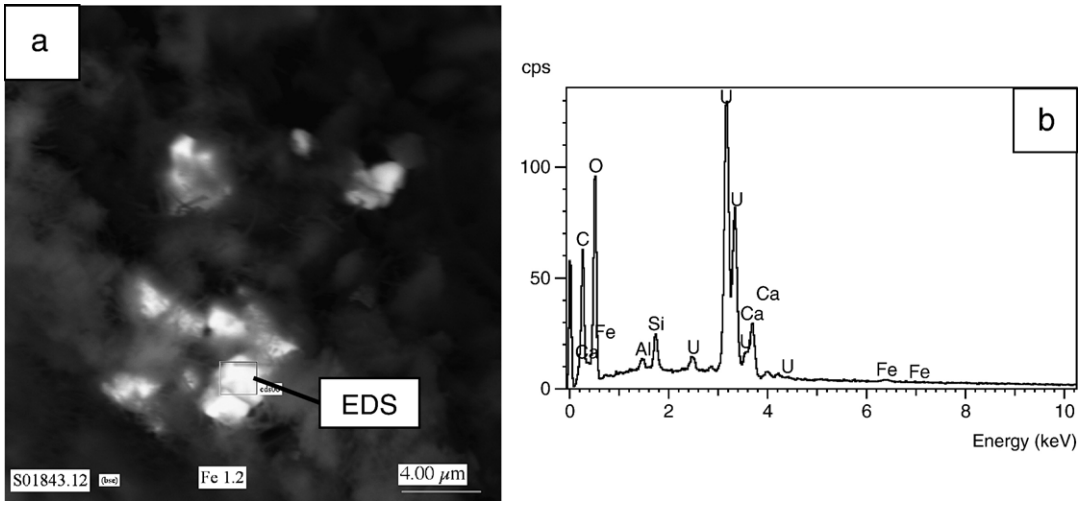

Fig. 5. (a) Scanning-electron photomicrograph of uranium phase formed within OPC spiked with 10^{-3} M uranium after one month. (b) Energy dispersive spectroscopic pattern indicates the phase is a mixed uranyl-oxide/silicate phase.

uranium-bearing precipitates after only two weeks. Fig. 6a and b demonstrate the formation of tabular-shaped, uranium-bearing precipitates embedded within the concrete matrix; additionally, cubic-shaped crystals are clearly identifiable in Fig. 6b. EDS analyses of the tabular-shaped precipitates provide a stoichiometric uranium:silica ratio of 2:1. The acicular morphology and stoichiometry of this phase are consistent with soddyite [$(UO_2)_2SiO_4(H_2O)_2$] (Fig. 6c). The cubic-shaped crystals contain calcium in addition to uranium, oxygen, and silica (Fig. 6d). The stoichiometry, in conjunction with morphological considerations, is suggestive of uranophane [$Ca(UO_2)_2(SiO_3OH)_2(H_2O)_5$] (Fig. 6d). Subsequent SEM–EDS analyses of concrete samples were conducted on monthly intervals. The occurrence of uranyl-oxyhydroxides decreased while the presence of uranyl-silicates increased after a period of one month. Stoichiometrically, uranyl-silicate compositions identified by EDS analyses remained suggestive of uranophane and soddyite phases and, this was corroborated by morphological observations from SEM analyses.

Fig. 7a and b illustrate SEM images of tabular uranium mineral precipitated *in situ* from 0.1 M uranium nitrate-spiked concrete within concrete sample composition five after two months. EDS

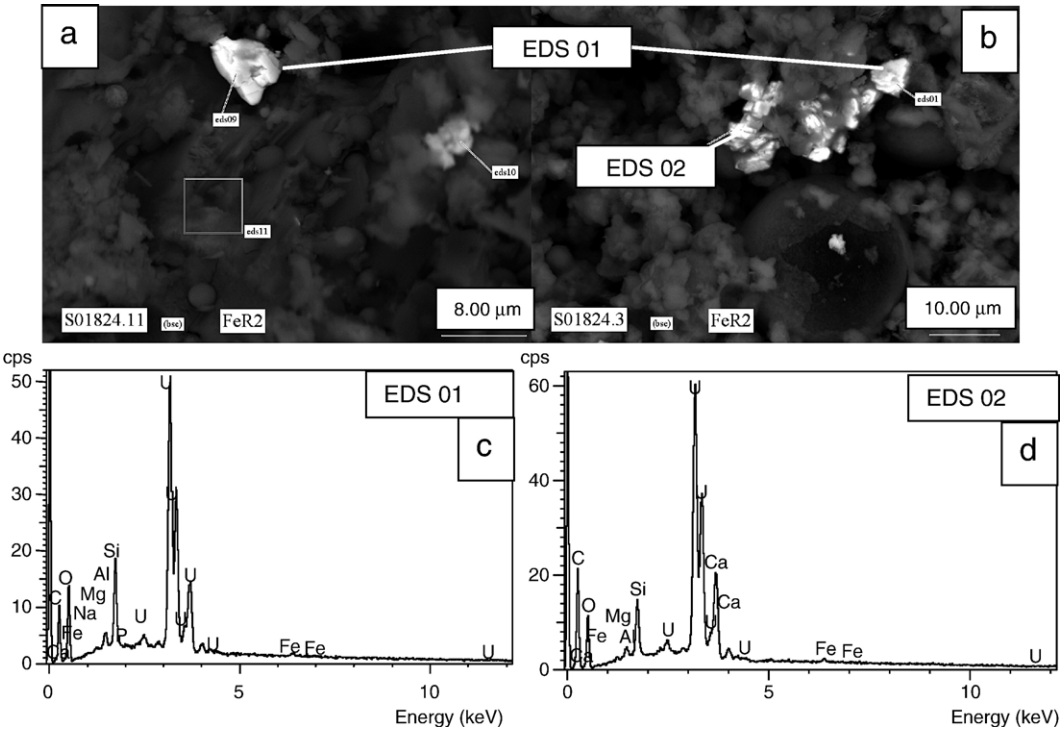

Fig. 6. (a) and (b) Scanning-electron photomicrographs of tabular uranium mineral precipitated *in situ* from 0.1 M uranium-spiked concrete after two weeks. (c) and (d) EDS analyses of tabular uranium precipitates. Results indicate the stoichiometry of the precipitates is consistent with uranium silicates: (c) EDS 01 is suggestive of soddyite, $(UO_2)_2SiO_4(H_2O)_2$ and d) EDS 02 is suggestive of uranophane, $Ca(UO_2)_2(SiO_3OH)_2(H_2O)_5$.

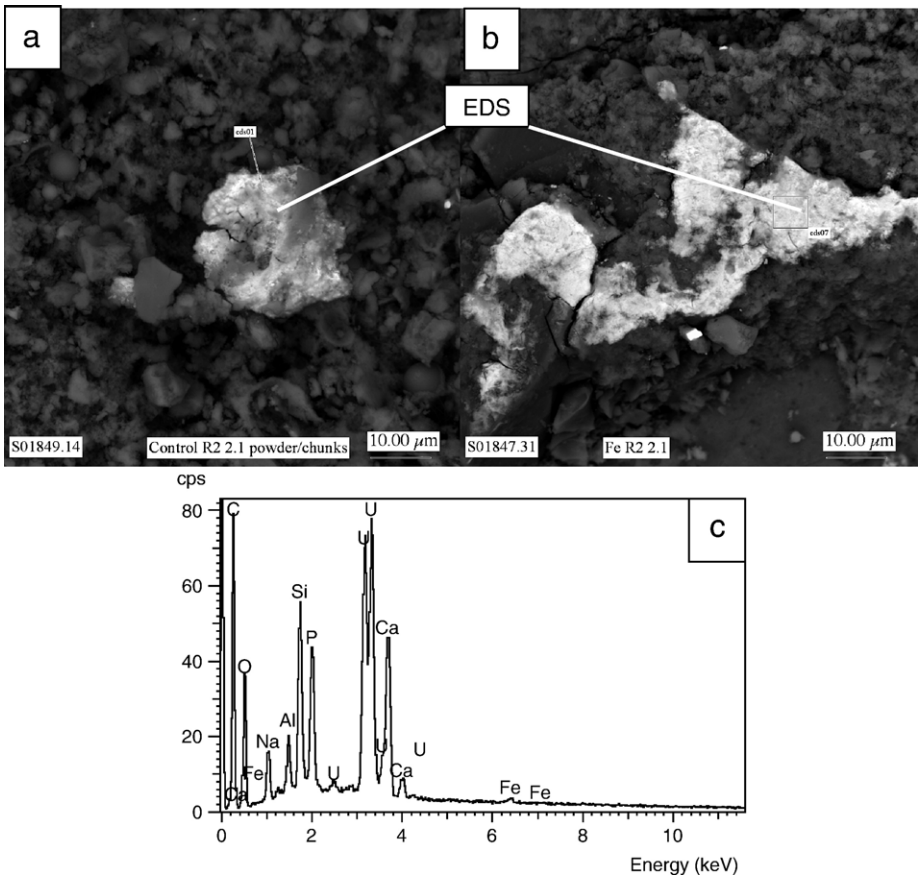

Fig. 7. (a) and (b) Scanning-electron photomicrographs of tabular uranium mineral precipitated *in situ* from 0.1 M uranium nitrate-spiked concrete within concrete sample composition five after two months. (c) EDS pattern corresponds to a mixed calcium-uranium-silicate/phosphate phase.

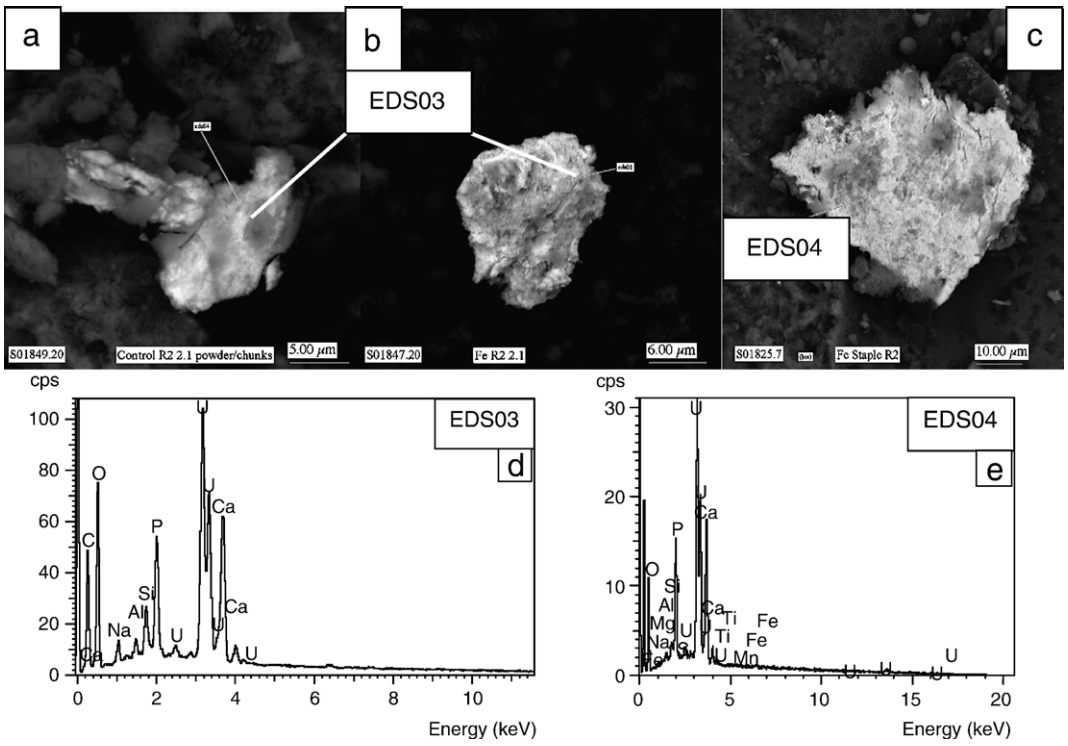

Fig. 8. (a–c) Scanning-electron photomicrographs of tabular uranium-phosphate phases formed within OPC spiked with 0.1 M uranium after two months. Phases exhibit morphology characteristic of autunite mineral. (d) and (e) EDS patterns indicates the stoichiometry is consistent with autunite, $Ca_2[(UO_2)_2(PO_4)_2]\cdot xH_2O$.

analyses of these regions indicate the coexistence of mixed uranium-silicate/phosphate phases (Fig. 7c). Morphologically, the mixed uranium-silicate/phosphate and uranium-phosphate regions appeared visually amorphous in SEM images (Fig. 7a and b). This is consistent with the fact that there are no known, naturally occurring, mixed uranyl-silicate/phosphate crystalline phases. However, it is possible that more detailed analyses may reveal structure on a nanoscopic scale wherein uranium-silicate and/or uranium-phosphate phases may be evident.

Fig. 8a–c illustrate regions of concentrated calcium-uranium-phosphate after a two month timeframe. In contrast to the mixed uranyl-silicate/phosphate phases, some structural definition of tabular-shaped morphology was evident in the uranyl-phosphate minerals. EDS analyses (Fig. 8d and e) demonstrate an increase in oxygen concentration with an increasing phosphorus concentration and concurrent decrease in silicon concentration. The overall stoichiometry approaches that consistent with autunite phases, $[Ca_2[(UO_2)_2(PO_4)_2]\cdot xH_2O]$.

The paragenesis of more soluble uranyl-oxyhydroxides to the more stable uranyl-silicate and uranyl-phosphate minerals is commonly observed in natural ore bodies [45,46] and areas with residual contamination from past nuclear activities undergoing natural attenuation [47–51]. However, this transformation has not been observed, nor has the potential occurrence been considered in the context of radioactive waste management. Compositionally, the concentration of phosphorus (predominantly from the fly ash component) within the concrete is approximately 10 ppm; whereas, the concentration of silica is nearly 200 ppm. However, as previously noted by Bogue [38] and Taylor [37], concrete is a continuously reacting solid, and its component phases continue to change over hundreds of years, albeit very slowly. This may allow diffusion and reaction of contaminants, such as uranium, within the matrix and, eventually, result in limited formation of more thermodynamically stable phases exhibiting long-term stabilization of uranium. Results presented here provide evidence, after one to three months, for all major divisions of the uranium paragenetic sequence (i.e., uranyl-oxyhydroxides, uranyl-silicates, and uranyl-phosphates). While, uranyl-silicate phases are the dominant uranyl minerals present within concrete matrices after a period of one month, depending on the composition of the concrete waste form, the presence of phosphorus may have significant implications for the long-term retention of uranium within the waste form.

4. Conclusions

Under ambient conditions, XRD data suggests diuranate salts, uranium-oxyhydroxides, and uranium-silicates are important in determining the solubility of uranium within concrete pore waters. However, uranium-oxyhydroxides and uranium-silicates are dominant uranium-solid phases present in thermally cured pore waters with increased crystallinity. These results support previous investigations suggesting the importance of uranium-oxyhydroxides, and to a limited degree, uranium-silicate minerals, on the retention of uranium within cementitious matrices. However, results of *in situ* characterization of uranium phases in concrete waste forms illustrate the interaction between components within the concrete matrix and uranium, affording significant control on the long-term solubility. Under conditions both under-saturated and over-saturated with respect to uranium-solid phases, uranium-solid phases were prevalent throughout concrete waste forms after two weeks. The significance of the uranium paragenetic sequence is also evident during the subsequent two-month time frame. Uranyl-oxyhydroxide phases were followed by the formation of mixed uranyl-oxyhydroxide/silicates, leading to the formation of uranyl-silicates, then mixed uranyl-silicate/phosphate and uranyl-phosphate phases. The importance of uranyl-phosphate minerals in concrete waste forms has, to date, been neglected because of the minimal amount of phosphorus present in most concrete compositions. However, because concrete is a continuously reacting solid, the thermodynamic stability of advanced uranyl minerals may have a substantial impact on the long-term fate of uranium.

Short-term batch tests conducted with concrete-equilibrated pore waters have frequently been utilized to identify the solubility-limiting phases controlling the long-term fate of contaminants immobilized in concrete waste forms. Results presented here illustrate the assumptions within this line of investigation may oversimplify the complexities of uranium chemistry especially when coupled with constantly changing conditions of concrete pore waters. Moreover, because coexisting solids of the concrete matrix are absent from the system, the system generally lacks buffering capacity and the influence of heterogeneous surfaces to promote nucleation of significant phases. Additionally, XRD results presented here for the identification of uranium phases precipitated from simulated concrete pore waters illustrate the significant challenges of discerning the solid phase(s) controlling the long-term solubility of uranium in complex matrices. The structural similarity of uranium-solid phases and formation of additional phases, such as calcium phases typically present in concrete, complicate interpretation of powder diffraction data. This precludes conclusive identification of solid phases precipitated from concrete pore waters based solely on XRD analyses and demonstrates the necessity to conduct multifaceted spectroscopic investigations to unambiguously identify solubility-limiting uranium phases. Future investigations should consider the potential benefit of including phosphorus in concrete waste forms and quantify the solubility of well-characterized uranium-solid phases under conditions relevant to concrete matrices.

Acknowledgements

This work was supported by Fluor Hanford and conducted at Pacific Northwest National Laboratory, operated by Battelle Memorial Institute for the U.S. Department of Energy under Contract DE-AC05-76RL01830.

References

[1] M.I. Wood, R. Khaleel, P.D. Rittman, A.H. Lu, S. Finfrock, R.J. Serne, K.J. Cantrell, Performance assessment for the disposal of low-level waste in the 218-W-5 burial ground, Westinghouse Hanford Company, WHC-EP-0645, 1995.

[2] F.M. Mann, R.J. Puigh, S.H. Finfrock, J. Freeman, R. Khaleel, D.H. Bacon, M.P. Bergeron, P.B. McGrail, S.K. Wurstner, Hanford immobilized

low-activity waste performance assessment: 2001 version, Pacific Northwest National Laboratory, DOE/ORP-2000-24, Rev. B, 2001.
[3] V.I. Plotnikov, V.I. Bannykh, Sorption of uranium(VI) by metal hydroxides.1. Sorption of uranium(VI) by tetravalent metal hydroxides, Radiochemistry 39 (1997) 158–161.
[4] V.I. Plotnikov, V.I. Bannykh, Sorption of uranium(VI) by metal hydroxides.2. Sorption of uranium(VI) by trivalent metal hydroxides, Radiochemistry 39 (1997) 162–164.
[5] V.I. Plotnikov, V.I. Bannykh, Sorption of uranium(VI) by metal hydroxides.3. Sorption of uranium(VI) by bivalent metal hydroxides and by mixed hydroxides of metals with different valence, Radiochemistry 39 (1997) 165–168.
[6] D.I. Kaplan, T.L. Gervais, K.M. Krupka, Uranium (VI) sorption to sediments under high pH and ionic strength conditions, Radiochim. Acta 80 (1998) 201–211.
[7] S.A. Carroll, J. Bruno, Mineral-solution and interactions in the U(VI)–CO_2–H_2O system, Radiochim. Acta 52/53 (1991) 187–193.
[8] S.A. Carroll, J. Bruno, J.C. Petit, J.C. Dran, Intractions of U(VI), Nd, and Th (IV) at the calcite–solution interface, Radiochim. Acta 58/59 (1992) 245–252.
[9] C.D. Tait, R.J. Reeder, J. Rakovan, D.E. Morris, E.J. Elzinga, D.J. Cherniak, M. Nugent, Abstracts of the papers of the American Chemical Society, J. Am. Chem. Soc. (2002).
[10] S.D. Kelly, M.G. Newville, L. Cheng, K.M. Kemner, S.R. Sutton, P. Fenter, N.C. Sturchio, C. Spotl, Uranyl incorporation in natural calcite, Environ. Sci. Technol. 37 (2003) 1284–1287.
[11] M.C. Duff, J. Urbanik-Coughlin, D.B. Hunter, Uranium co-precipitation with iron oxide minerals, Geochim. Cosmochim. Acta 66 (2002) 3547–3553.
[12] M. Rovira, F.Z.E. Aamrani, L. Duro, I. Casas, J.d.J. Pablo, C. Bruno, C. Domenech, Experimental study and modeling of uranium (VI) transport through ferrous olivine rock columns, Radiochim. Acta 88 (2000) 665–671.
[13] M.A. Denecke, J. Rothe, K. Dardenne, P. Lindqvist-Reis, Grazing incidence (gi) XAFS measurements of Hf(IV) and U(VI) sorption onto mineral surfaces, Phys. Chem., Chem. Phys. 5 (2003) 939–946.
[14] J.D. Prikryl, A. Jain, D.R. Turner, R.T. Pabalan, Uranium(VI) sorption behavior on silicate mineral mixtures, J. Contam. Hydrol. 47 (2001) 241–253.
[15] L.P. Moroni, F.P. Glasser, Reactions between cement components and U(VI) oxide, Waste Manag. 15 (1995) 243–254.
[16] B. Kienzler, B. Luckscheiter, S. Wilhelm, Waste form corrosion modeling comparison with experimental results, Waste Manag. 21 (2001) 741–752.
[17] S.L. Matzen, J.M. Beiriger, P.C. Torretto, P. Zhao, B.E. Viani, Uranium (VI) and neptunium(V) transport through fractured, hydrothermally altered concrete, Radiochim. Acta 88 (2000) 657–664.
[18] C. Altenhein-Hasse, H. Bischoff, L. Fu, J. Mao, G. Marx, Adsorption of actinides on cement compounds, J. Alloys Compd. 213/214 (1994) 554–556.
[19] E.R. Sylwester, P.G. Allen, P. Zhao, B.E. Viani, Interactions of uranium and neptunium with cementitious materials studied by XAFS, Lawrence Livermore National Laboratory, UCRL-JC-135988, 1999.
[20] G. Sposito, The Chemistry of Soils, Oxford University Press, New York, NY, 1989.
[21] M. Sutton, P. Warwick, A. Hall, Uranium (VI) interactions with OPA/PFA grout, R. Soc. Chem. 5 (2003) 922–928.
[22] R.J. Serne, W.J. Martin, V.L. LeGore, C.W. Lindenmeier, S.B. McLaurine, P.F.C. Martin, R.O. Lokken, Leach tests on grouts made with actual and trace metal-spiked synthetic phosphate/sulfate waste, Pacific Northwest Laboratory, PNL-7121, 1989.
[23] R.J. Serne, R.O. Lokken, L.J. Criscenti, Characterization of grouted llw to support performance assessment, Waste Manag. 12 (1992) 271–287.
[24] R.J. Serne, L.L. Ames, P.F. Martin, V.L. LeGore, C.W. Lindenmeier, S.J. Phillips, Leach testing of in situ stabilization grouts containing additives to sequester contaminants, Pacific Northwest Laboratory, PNL-8492, 1992.
[25] R.J. Serne, W.J. Martin, V.L. LeGore, Leach test of cladding removal waste grout using Hanford groundwater, Pacific Northwest Laboratory, PNL-10745, 1995.
[26] R.J. Serne, A.T. Owen, C.W. Lindenmeier, Solubility of U(VI) in sorbond LPC II solidified waste from 183-H basin, Pacific Northwest National Laboratory, PNL-11183, 1996.
[27] R.J. Serne, D. Rai, P.F. Martin, A.R. Felmy, L. Rao, S. Ueta, Scientific basis for nuclear waste management XIX, Pittsburgh, Pennsylvania, 1996, Materials Research Society, 1996.
[28] K.M. Krupka, R.J. Serne, Performance assessment of low-level radioactive waste disposal facilities: effects on radionuclide concentrations by cement/ground–water interactions, U.S. Nuclear Regulatory Commission, NUREG/CR-6377, 1996.
[29] M. Sutton, Uranium Solubility, Speciation and Complexation at High pH. Loughborough University, Ph.D. Dissertation (1999).
[30] M. Sutton, P. Warwick, A. Hall, C. Jones, Carbonate induced dissolution of uranium containing precipitates under cement leachate conditions, J. Environ. Monit. 1 (1999) 177.
[31] M. Brownsword, A.B. Buchan, F.T. Ewart, Materials Research Symposium Society Proceedings, 1990, 1990.
[32] M. Atkins, A.N. Beckley, F.P. Glasser, Influence of cement on the near field environment and its specific interactions with uranium and iodine, Radiochim. Acta 44/45 (1988) 255–261.
[33] F.P. Glasser, A.A. Rahman, D. Macphee, M.J. Angus, M. Atkins, Immobilization of Radioactive Waste in Cement-Based Matrices, University of Aberdeen, 1985 DOE/RW/85.189.
[34] F.P. Glasser, Mineralogical aspects of cement in radioactive waste disposal, Mineral. Mag. 65 (2001) 621–633.
[35] P. Zhao, P.G. Allen, E.R. Sylwester, B.E. Viani, The partitioning of uranium and neptunium onto hydrothermally altered concrete, Lawrence Livermore National Laboratory, URCL-JC-136032, 1999.
[36] M.J. Cooper, D.P. Hodgkinson, UKAEA Report NSS/R101, 1987.
[37] H.F.W. Taylor, Cement Chemistry, Academic Press, New York, 1990.
[38] R.H. Bogue, Chemistry of Portland Cement, Reinhold Publishing Corporation, New York, 1955.
[39] F.T. Ewart, J.L. Smith-Briggs, H.P. Thonason, S.J. Williams, The solubility of actinides in a cementitious near-field environment, Waste Manag. 12 (1992) 241–252.
[40] T. Yamamura, A. Kitamura, A. Fukui, S. Nishikawa, T. Yamamoto, H. Moriyama, Solubility of U(VI) in highly basic solutions, Radiochim. Acta (1998) 139–146.
[41] B.P. Spalding, Volatility and extractability of strontium-85, cesium-134, cobalt-57, and uranium after heating hardened portland cement paste, Environ. Sci. Technol. 34 (2000) 5051–5058.
[42] T. Reich, H. Moll, M.A. Denecke, G. Geipel, G. Bernhard, H. Nitsche, P.G. Allen, J.J. Bucher, N. Kaltsoyannis, N.M. Edelstein, D.K. Shuh, Radiochim. Acta 74 (1996) 219.
[43] E.A. Hudson, L.J. Terminello, B.E. Viani, M.A. Denecke, T. Reich, P.G. Allen, J.J. Bucher, D.K. Shuh, N.M. Edelstein, Clays Clay Miner. 47 (1999) 439.
[44] E.R. Sylwester, E.A. Hudson, P.G. Allen, The structure of uranium (VI) sorption complexes on silica, alumina, and montmorillonite, Geochim. Cosmochim. Acta 64 (2000) 2431–2438.
[45] R.J. Finch, R.C. Ewing, The corrosion of uraninite under oxidizing conditions, J. Nucl. Mater. 190 (1992) 133–156.
[46] T. Murakami, T. Ohnuki, H. Isobe, T. Sato, Mobility of uranium during weathering, Am. Mineral. 82 (1997) 888–899.
[47] E.C. Buck, N.R. Brown, N.L. Dietz, Contaminant uranium phases and leaching at the Fernald Site in Ohio, Environ. Sci. Technol. 30 (1996) 81–88.
[48] V.C. Tidwell, D.E. Morris, J.C. Cunnane, S.Y. Lee, Characterizing soils contaminated with heavy metals: a uranium contamination case study, Rem. J. (1996) 81–96.
[49] S.Y. Lee, J.D. Marsh, Characterization of uranium-contaminated soils from DOE Fernald Environmental Management Project site: results of phase I characterization, Oak Ridge National Laboratory, ORNL/TM-11980, 1992.
[50] M.P. Elless, S.Y. Lee, Uranium solubility of carbonate-rich uranium-contaminated soils, Water Air Soil Pollut. 107 (1998) 147–162.
[51] M.P. Elless, S.Y. Lee, Physicochemical and mineralogical characterization of transuranic contaminated soils for uranium soil integrated demonstration, Oak Ridge National Laboratory, ORNL/TM-12848, 1994.